frontiers | Frontiers in Marine Science

TYPE Original Research
PUBLISHED 01 December 2022
DOI 10.3389/fmars.2022.1080516

OPEN ACCESS

EDITED BY
Li Zhang,
South China Sea Institute of Oceanology, Chinese Academy of Sciences (CAS), China

REVIEWED BY
Jinling Cao,
Shanxi Agricultural University, China
Xinguo Zhao,
Yellow Sea Fisheries Research Institute, Chinese Academy of Fishery Sciences (CAFS), China

*CORRESPONDENCE
Alan Kueichieh Chang
akcchang@163.com
Xueping Ying
xpying2008@wzu.edu.cn

†These authors have contributed equally to this work

SPECIALTY SECTION
This article was submitted to Marine Pollution, a section of the journal Frontiers in Marine Science

RECEIVED 26 October 2022
ACCEPTED 16 November 2022
PUBLISHED 01 December 2022

CITATION
Bai B, Yang Y, Wei J, Zheng Q, Wang M, Chang AK and Ying X (2022) Cadmium-induced toxicity in *Meretrix meretrix* ovary is characterized by oxidative damage with changes in cell morphology and apoptosis-related factors. *Front. Mar. Sci.* 9:1080516. doi: 10.3389/fmars.2022.1080516

Cadmium-induced toxicity in *Meretrix meretrix* ovary is characterized by oxidative damage with changes in cell morphology and apoptosis-related factors

Binbin Bai[1†], Yuqing Yang[1†], Jinyan Wei[1], Qi Zheng[1], Mengci Wang[1], Alan Kueichieh Chang[1*] and Xueping Ying[1,2*]

[1]College of Life and Environmental Sciences, Wenzhou University, Wenzhou, Zhejiang, China, [2]National and Local Joint Engineering Research Center of Ecological Treatment Technology for Urban Water Pollution, Wenzhou University, Wenzhou, Zhejiang, China

Cadmium (Cd) is one of the most common pollutants in the environment. It can cause irreversible tissue damage and apoptosis in invertebrates. This study investigated the relationship between Cd exposure and oxidative damage and apoptosis in the ovarian cell of the clam *Meretrix meretrix*. The clams were exposed to different concentrations of Cd^{2+} (0, 1.5, 3, 6 and 12 mg L^{-1}) for 5 days, and the accumulated level of Cd^{2+} in the ovarian tissue, and the degree of oxidative damage, changes in morphology and the response of apoptosis-related factors in the ovarian cell were determined. The bioaccumulation of Cd^{2+} and the levels of reactive oxygen species (ROS), malondialdehyde (MDA), protein carbonylation (PCO), and DNA-protein crosslinking (DPC) in the ovary were found to increase significantly when the clams were exposed to increasing concentrations of Cd^{2+}. The structure of the ovarian tissue was severely damaged, and the ovarian cells displayed an irregular arrangement. The results of AO/EB staining and flow cytometry showed that the apoptotic rate of the ovarian cells increased with increasing Cd^{2+} concentrations. The activities of caspase-3, -8, -9, and the mRNA levels of *p53*, *Bax* and *Caspase-3* in the ovary were also significantly increased. Furthermore, the level of *p53* mRNA was positively correlated with the levels of MDA, PCO, DPC and ROS, but negatively correlated with the levels of total antioxidant capacity (T-AOC) and *Bcl-2* mRNA. Taken together, these results indicated that Cd^{2+} exposure would result in oxidative damage and apoptosis for the ovarian cells, suggesting that Cd^{2+} toxicity could negatively affect the reproductive capacity of *M. meretrix*, thus threatening the reproductive development of the shellfish.

KEYWORDS

***Meretrix meretrix*, cadmium, ovary, oxidative damage, apoptosis-related factors**

1 Introduction

With the rapid development of industry and agriculture, the environment of coastal water has been seriously polluted. In particular, heavy metal pollution has seriously affected the growth and development of marine organisms, with the potential of causing death to the organisms. Previous research has shown that heavy metals are highly toxic to aquatic animals, with Cd, Zn, Pb and Cu toxicity being a major cause of death (Garriz et al., 2019; Chen et al., 2020; Zhan et al., 2021). Cadmium (Cd) that enters the tissue of aquatic animals, such as *Penaeus vannamei* (Nunez-Nogueira et al., 2012), *Danio rerio* (Wu et al., 2012), *Eriocheir sinensis* (Lin et al., 2017) and *Crassostrea gigas* (Cao et al., 2018), can cause a series of toxicological reactions that lead to irreversible biological damage. It also acts as a peroxidation inducer that promotes the production of a high level of reactive oxygen species (ROS) (Wang et al., 2021). When the amount of ROS exceeds the capacity of the organism to clear it, it will result in membrane lipid peroxidation, protein carbonylation (PCO), and DNA-protein crosslinking (DPC) (Jena, 2012; Fedorova et al., 2014; Zhang et al., 2016). Malondialdehyde (MDA), a lipid peroxide, can be used as a marker to assess the degree of lipid peroxidation in the body (Tirani and Haghjou, 2019). PCO can lead to protein degradation and the carbonylation of a specific protein will affect the downstream cellular events mediated by that protein, whereas DPC can interrupt nearly all DNA metabolic processes. Thus, increases in MDA, PCO and DPC levels will lead to oxidative damage and apoptosis (Xie et al., 2007; Sevcikova et al., 2011; Boudet et al., 2015).

In the process of evolution, organisms have evolved effective antioxidant systems, which can scavenge ROS and its metabolites. The role of total antioxidant capacity (T-AOC) in the defense system is to maintain the dynamic balance of ROS in the internal environment by removing excess ROS to keep the organism in a relatively stable redox state. Therefore, T-AOC is an index that comprehensively reflects the ability of tissues to resist the damage inflicted by ROS (Sarban et al., 2005; Cekic et al., 2013). Metallothionein (MT) is a low molecular weight metal-binding protein rich in cysteine. MT can bind with heavy metals, effectively scavenging the heavy metals to adjust the concentration of heavy metal ions in the cells, reduce the toxic effects of heavy metals on the body and protect organelles from heavy metal-inflicted damage. Thus, MT has a strong ability to detoxify heavy metals by acting as an antioxidant (Wu et al., 2006; Gu et al., 2019). MT synthesis is induced by metal contaminants (e.g., Ag, Cd, Cu, and Hg) in many species (e.g., annelids, molluscs, crustaceans, and fish), suggesting the potential use of MT concentration as an indicator of metal exposure in organisms (Amiard et al., 2006). In addition, MT has been shown to play an important role in the apoptosis pathway, where it can inhibit apoptosis by inhibiting the release of mitochondrial cytochrome c and the activation of caspase-3 (Wang et al., 2001).

P53 and caspase (Cysteine-requiring Aspartate Protease) are two important factors in cell apoptosis (Wang et al., 2001; Wang et al., 2011; Ostrakhovitch et al., 2016). p53 is one of the most common pro-apoptotic proteins. It can arrest cell proliferation at the G1 phase and is a key factor for cell apoptosis and cell arrest (Brady and Attardi, 2010; Ostrakhovitch et al., 2016). P53 induces apoptosis through the expression of pro-apoptotic proteins (e.g., Bax) and inhibits the expression of anti-apoptotic proteins (e.g., Bcl-2) (Brady and Attardi, 2010). Caspase is a member of the protease family that plays a key role in apoptosis. Caspase-3 is an executioner caspase that triggers apoptosis through down-regulating or even inactivating enzymes involved in DNA repairs (Wang et al., 2001; Wang et al., 2011). Caspase-8 and caspase-9 are initiator caspases, and both can activate caspase-3. Caspase-8 activates caspase-3 *via* the extrinsic pathway while caspase-9 does it through the intrinsic pathway (Kumar, 2007; Kim et al., 2015; Tummers and Green, 2017). Despite the overwhelming amount of research on apoptosis, the roles of these apoptotic factors in the apoptotic pathway of bivalves induced by cadmium are not clear.

Bivalves are one of the important groups of marine animals in the aquatic ecosystem, and *M. meretrix* (Bivalvia, Veneridae) is one of the economically important bivalves in China. Its benthic lifestyle makes it susceptible to the accumulation of toxic metals in the aquatic environment, and therefore, it is considered an indicator of toxic metal pollution in the aquatic environment (Alyahya et al., 2011). Cadmium is one of the important heavy metals found as a pollutant in the sea. Cadmium can affect the formation and development of aquatic animal germ cells, causing oxidative damage and apoptosis in ovarian cells (Chen et al., 2019; Das et al., 2013; Revathi et al., 2011; Xu et al., 2016). Bivalves release mature germ cells into the aquatic environment for fertilization, and this can make the released germ cells more sensitive to the heavy metals in the water. Therefore, it is very important to study and evaluate the extent of damage inflicted by Cd toxicity in the reproductive tissue of the bivalves exposed to this metal. Cadmium may reduce the fecundity of aquatic organisms, thus adversely affecting the structure of the aquatic ecosystem and the integrity of shellfish farming. Although the concentration of cadmium in the aquatic environment is not high, the exposure time to cadmium is very long, and such long exposure could lead to increased accumulation of cadmium in the aquatic organisms with time (Chen et al., 2020). Exploring the relationship between Cd and apoptosis of shellfish not only can enrich the research of environmental toxicology but can also enable us to better understand the mechanism of cellular toxicology in shellfish. At the same time, it also has significance in the sustainable development of aquaculture and the protection of economically

viable marine animal resources. In this study, the toxicity of Cd in *M. meretrix* ovary was evaluated to gain more insight into the toxicological mechanism of cadmium in ovarian cell apoptosis.

2 Materials and methods

2.1 Animals and treatments

Meretrix meretrix individuals (shell length, 46.52 ± 0.28 mm; shell width, 23.51 ± 0.22 mm; shell height, 37.73 ± 0.21 mm; weight, 27.25 ± 0.22 g) were purchased in July 2020 from Lingkun aquafarm, Wenzhou, Zhejiang, China. The seawater of the aquafarm where the clams were raised had a Cd^{2+} concentration of 0.54 μg L^{-1}, which is within the Chinese standard for first-class seawater quality. The clams were randomly assigned to five groups and each group was exposed to a different Cd^{2+} concentration (0, 1.5, 3, 6, or 12 mg L^{-1}). These concentrations of Cd^{2+} correspond to 1/10, 1/5, 1/2.5, and 1/1.25 of the LC_{50} (15.01 mg L^{-1}) previously determined from a 4-day Cd^{2+} exposure (Xia et al., 2016). Each group consisted of 120 clams that were kept in three separate aquariums, with 40 clams per aquarium. The clams were exposed to the Cd^{2+} solutions without food for 5 days at 22 ± 1°C and pH 8.0. A 5-day exposure was used instead of a 4-day exposure to maximize the effect of the Cd exposure, and at the same time without killing the clams, since prolonged exposure to 12 mg L^{-1} Cd^{2+} has been found to result in inactivity and even death for the clams. The aquaculture water in each aquarium was replaced daily with fresh water (prepared from double distilled water and artificial seawater salt) containing the same Cd^{2+} concentration. At the end of the exposure period, all clams were dissected, and the ovaries were quickly removed from the female clams and processed according to the following experiments. All animal experimental procedures used complied with the Wenzhou University Animal Care and Use Committee's (WU-ACUC) guidelines, and this experiment was approved by the WU-ACUC.

2.2 Determination of Cd in the ovary of the clam

To determine the Cd^{2+} content of the ovary, two female clams were randomly selected from each aquarium (sample size = 6/treatment) to harvest their ovaries. The concentration of Cd^{2+} in the ovary was measured following the experimental methods of Lin et al. (2017).

2.3 Detection of oxidative damage indicators

Two clams were randomly taken from each aquarium (sample size = 6/treatment) and their ovaries were extracted and then homogenized in 9 vol of 0.9% ice-cold physiological saline using a high throughput tissue grinder (SCIENTZ-48, China) kept on ice. The homogenate was then centrifuged at 12000 × *g* and 4°C for 5 min and the supernatant was retained, yielding an ovary extract. The levels of MDA, PCO, DPC, ROS and T-AOC in the ovary extract were then measured as described below.

2.3.1 MDA assay

MDA content was measured with an MDA assay kit (Nanjing Jiancheng Biological Engineering Institute) according to the manufacturer's instructions. MDA released from the degradation of lipid peroxide can react with thiobarbituric acid (TBA) under high temperatures and an acidic environment to produce a reddish-brown product, trimethadione (3, 5, 5-Trimethyloxazolidine-2, 4 - dione), which has a maximum absorption at 532 nm. MDA level was expressed in nmol per mg protein (nmol mg^{-1}).

2.3.2 PCO content assay

The content of PCO in the ovary was measured using DNPH (2, 4-dinitrophenylhydrazine) as described by Xie et al. (2007). The carbonyl group on the protein would react with DNPH to form a red precipitate, 2, 4-dinitrophenylhydrazone, which is soluble in guanidine hydrochloride and has a characteristic absorption peak at 370 nm. The PCO content was calculated according to the absorbance at 370 nm and expressed as nmol per mg protein (nmol mg^{-1}).

2.3.3 DPC assay

DPC was determined by the SDS precipitation method according to Xie et al. (2007). Briefly, cells were lysed with 2% SDS and the proteins (including free proteins and protein-DNA complexes) from the cell lysate were precipitated by centrifugation. The protein precipitate was then digested with proteinase K to collect the DNA in the protein-DNA complex (bind-DNA). The absorbance values of free-DNA and protein-bound DNA were measured using Hoechst 33258 fluorescent dye. The result was expressed as the percentage (DPC coefficient) of bound DNA to total DNA (free-DNA plus bind DNA).

2.3.4 ROS assay

ROS production was measured with a ROS Assay Kit (Beyotime Institute of Biotechnology, Shanghai, China), which measured the level of DCFH-DA (2, 7-Dichlorodihydrofluorescein diacetate), an indicator of oxidative stress. After entering the cell, DCFH-DA is rapidly oxidized to generate a strong fluorescent product, DCF (2', 7'-dichlorofluorescein), which can then be detected by fluorescence using an excitation wavelength of 488 nm and an emission wavelength of 525 nm.

2.3.5 T-AOC assay

T-AOC level was measured using the ABTS method with 2, 2'-azino-bis (3-ethylbenzothiazoline-6-sulfonic acid) (ABTS) as performed with a T-AOC assay kit (Nanjing Jiancheng Biological Engineering Institute, Nanjing, China). The assay is based on the oxidation of ABTS to $ABTS^{+}$ (green) by oxidants present in the ovary homogenate. However, when an antioxidant is present, the production of $ABTS^{+}$ is inhibited, leading to a decrease in absorbance at 734 nm. T-AOC level was expressed in mmol per g protein (mmol g^{-1}).

2.4 Histological evaluation

The morphological changes of the ovary after Cd^{2+} treatment were observed by Hematoxylin-eosin (H&E) staining. One clam was randomly taken from each aquarium (sample size = 3/treatment) and its ovary was extracted and immobilized in 4% (v/v) paraformaldehyde for 24 h, followed by dehydration in different concentrations of ethanol (75%, 85%, 90%, 95% and 100%). The dehydrated samples were embedded in melted paraffin and sectioned with a microtome (YD-315, China) to yield 7-μm thick slices. The slices were then deparaffinized, dehydrated, stained with hematoxylin and eosin, and finally sealed with neutral balsam and observed with a light microscope (Olympus BX51, Japan).

2.5 Detection of apoptosis

2.5.1 Acridine orange/ethidium bromide staining

The degree of damage to the ovary induced by Cd^{2+} was examined by AO/EB staining carried out according to the method described by Xia et al. (2016). Two clams were randomly taken from each aquarium (sample size = 6/treatment) and their ovaries were extracted. About 80 mg of the ovarian tissue was made into a cell suspension in 1% precooled PBS (pH = 7.2). An aliquot (25 μL) of the cell suspension was mixed with 1 μL AO/EB solution (100 μg mL^{-1} of AO in PBS; 100 μg mL^{-1} of EB in PBS) and incubated for 5 min and then examined under a fluorescence microscope (Nikon Ti-s, Japan).

2.5.2 Annexin V-FITC/PI staining by flow cytometry

Ovaries were extracted from two clams randomly taken from each aquarium (sample size = 6/treatment). The ovaries were washed with 15 ‰ seawater to obtain an ovarian cell suspension with a final concentration of 1×10^{6} cells mL^{-1}. An aliquot (100 uL) of the cell suspension was taken from each preparation and mixed with 900 μL seawater. After that, 1 mL of the diluted cell suspension was divided into four centrifuge tubes (250 μL each tube) and centrifuged at 2500 × *g* and 4°C for 5 min. The supernatant from each tube was removed and the precipitate was mixed with 100 μL buffer. The first tube was kept as a blank (no addition of dye). In the second tube was added 5 μL Annexin V-FITC whereas in the third tube was added 5 μL PI. In the fourth tube was added 5 μL Annexin V-FITC and 5 μL PI. After the addition of the dyes, the samples were gently swirled to mix and then incubated for 15 min at room temperature in the dark, followed by the addition of 400 μL 1× Binding Buffer and gentle mixing. The cells were then immediately analyzed by flow cytometry (BD FACSCantoII, San Jose, USA). The results were expressed as Annexin V-FITC/PI dot plots. For each sample, a total of 10,000 cells were counted for statistical analysis.

2.5.3 Caspase activity assay

Caspase-3, caspase-8 and caspase-9 activity levels in the ovary were measured using commercial kits (Beyotime, Shanghai, China) according to the manufacturer's instructions. Briefly, two clams from each aquarium (sample size = 6/treatment) were randomly collected and the ovary of each clam was then extracted. After that, 10 mg of the ovary was mixed with 100 μL lysis buffer provided in the kit and homogenized using a pre-cooled high throughput tissue grinder (SCIENTZ-48, China). The homogenate was then centrifuged at 16,000 × *g* and 4°C for 12 min, and the supernatant was subjected to caspase-3, -8 and -9 assays using the corresponding assay kits.

2.6 Analysis of p53, MT, Bax, Bcl-2 and Caspase-3 mRNA

Total RNA was extracted from the ovaries extracted from two clams randomly taken from each aquarium (sample size = 6/treatment). The RNA was extracted using a UNIQ-10 column Trizol Total RNA Extraction Kit (Shanghai Sangon, China) according to the manufacturer's protocol. The quality of the RNA was evaluated by agarose gel electrophoresis, while its content was determined by UV spectrophotometry. The extracted RNA was reverse transcribed into cDNA using PrimeScript RT Reagent Kit (TaKaRa) according to the manufacturer's instructions, and 1 μg of RNA was used as a template in a 20 μL reaction. RT-PCR was performed on a Roche LC480 PCR instrument (Switzerland) using a TB Green PCR kit (TaKaRa, Dalian, Liaoning, China) with *β-actin* as the housekeeping gene. The qPCR primers for *p53*, *MT*, *Bax*, *Bcl-2*, *caspase-3* and *β-actin* genes are listed in Table 1. The PCR conditions were as follows: an initial step at 95°C for 5 min followed by 40 cycles of 15 s at 95°C, 15 s at 58°C, and 20 s at 72°C. The relative expression level was calculated by using the $2^{-\Delta\Delta Ct}$ method (Livak and Schmittgen, 2001; Huang et al., 2020).

2.7 Statistical analysis

Statistical analysis of the data was performed with the SPSS Statistical Package (Version 23.0, Chicago, USA) and Origin

TABLE 1 Primers used for qRT-PCR.

Primer name	Sequence (5' to 3')	Tm value	Product length	Genbank No.
p53-F	GTTCCCACTGTACCATCGAATA	53°C	100 bp	MK270123.1
p53-R	ACGTCCAGGTGGTTGATTT	57°C		
MT-F	CGAGGACTGTTCATCAACCACTG	59°C	91 bp	GU233466.1
MT-R	GCAAACAACTTTACACCCTGGAC	59°C		
Bax-F	TTGCCAACGATTTCTTCCG	53°C	203 bp	ON040963
Bax-R	CATTTCCCAGCCACCTCTC	59°C		
Bcl-2-F	AGACAATGGTGGCTGGGATG	59°C	122 bp	ON040964
Bcl-2-R	CGGCAGCTAATGCTCCAAGA	56°C		
caspase-3-F	GAAGCCAGCAAGTGCACAAAC	59°C	117 bp	ON040965
caspase-3-R	GCAAGCATGTACCCTCGTTG	59°C		
β-actin-F	TTGTCTGGTGGTTCAACTATG	55°C	175 bp	JN084197.1
β-actin-R	TCCACATCTGCTGGAAGGTG	59°C		

Statistical Package (Version 9.2, Northampton, USA). All data were expressed as means ± standard errors (mean ± S.E.). Significance differences between the control group and treatment groups were determined using a one-way ANOVA. In addition, correlation analysis was performed with Pearson Correlation Coefficient using SPSS 23.

3 Results

3.1 Cd bio-accumulation in *M. meretrix* ovary

The Cd^{2+} level for the control group was 0.338 ± 0.009 mg kg^{-1} wet tissue whereas the Cd^{2+} levels for the groups treated with 1.5, 3, 6, 12 mg L^{-1} Cd^{2+} were 1.696 ± 0.010, 2.443 ± 0.012, 3.350 ± 0.012, and 4.637 ± 0.061 kg^{-1} wet tissue, respectively. All Cd^{2+}-treated groups exhibited a significant (P<0.05) increase in accumulated Cd^{2+} in the ovary compared with the control, with the group treated with 12 mg L^{-1} Cd^{2+} displaying the maximum Cd^{2+} level. The accumulated Cd^{2+} level in the ovary of the clams clearly showed a dose-response relationship with respect to the concentration of Cd^{2+} in the water that the clams were exposed to.

3.2 Detection of oxidative damage indexes

3.2.1 Effects of Cd on MDA, PCO and DPC contents

The levels of MDA, PCO and DPC in the ovary increased when *M. meretrix* was exposed to rising Cd^{2+} concentrations (Figures 1A–C). The MDA level in the control group was not significantly ($P > 0.05$) different from those of the groups treated with lower Cd^{2+} concentrations (1.5 and 3 mg L^{-1}) but was significantly ($P < 0.05$) lower than those of the groups treated with higher Cd^{2+} concentrations (6 and 12 mg L^{-1}) (Figure 1A). The PCO level in the control group was not significantly different ($P > 0.05$) from the group treated with 1.5 mg L^{-1} Cd^{2+}, but it was significantly ($P < 0.05$) lower than those of the groups treated with 3, 6 and 12 mg L^{-1} Cd^{2+} (Figure 1B). However, the DPC level of the control group was significantly ($P < 0.05$) lower than that of each Cd^{2+}-treated group (Figure 1C). Overall, Cd^{2+} seemed to induce the production of MDA, PCO and DPC as part of its toxic effect.

3.2.2 Effects of Cd^{2+} on ROS and T-AOC contents

The content of ROS in the ovary of Cd^{2+}-treated *M. merertrix* increased with increasing Cd^{2+} concentrations, but a significant ($P < 0.05$) increase over the control group was observed only for the groups treated with 6 and 12 mg L^{-1} Cd^{2+} (Figure 1D, white bars). T-AOC content in the ovary showed a slight but significant increase over the control group for the group treated with the lowest Cd^{2+} concentration (1.5 mg L^{-1}) but then decreased to a level significantly lower than that of the control group with further increases in Cd^{2+} concentration (Figure 1D, black bars). These results indicated that Cd^{2+} led to ROS accumulation in the ovary, resulting in oxidative damage, and exposure to a high Cd^{2+} concentration may overwhelm the intracellular antioxidant capacity of the ovarian cells.

3.3 Morphological changes of ovarian tissue after Cd^{2+} treatment

The effect of Cd^{2+} on the tissue structure of *M. meretrix* ovary was observed by light microscopy. In the control group, the gonadal structure was complete, the ovarian cells had a normal shape and were tightly arranged, and the number of follicular epithelial cells was higher compared with those of the

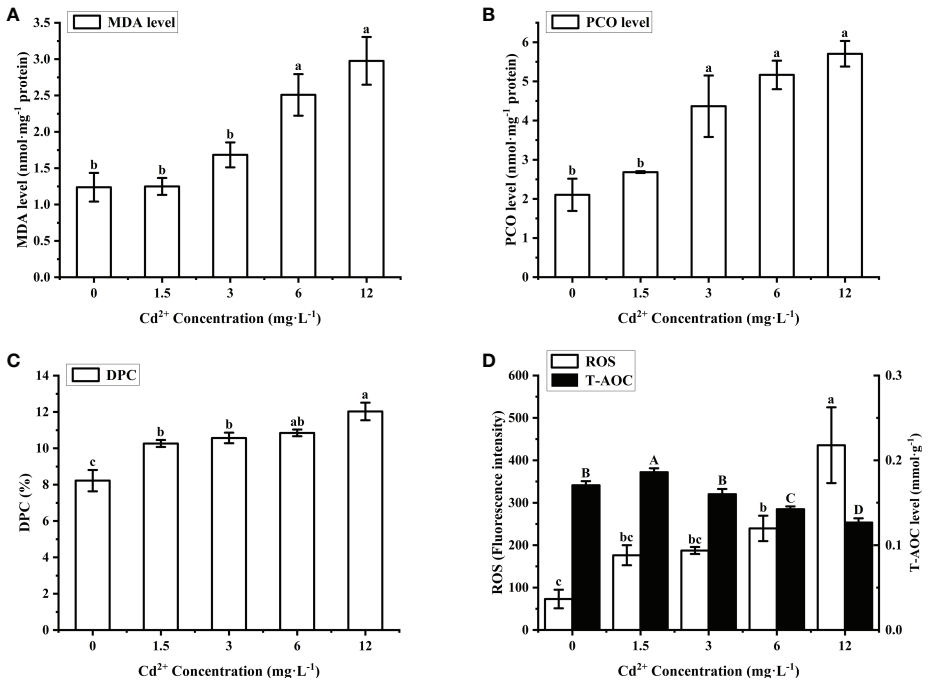

FIGURE 1
Effects of Cd on MDA, DPC, PCO, ROS and T-AOC in *M. meretrix* ovary. **(A)** MDA level; **(B)** PCO level; **(C)** DPC level; **(D)** ROS (white bars) and T-AOC (black bars) contents. Different letters indicate significant ($P < 0.05$) differences among groups as revealed by Tukey's post-hoc multiple comparison tests; Data are expressed as means ± SE (n = 6).

Cd^{2+}-treated groups (Figure 2A). In the Cd^{2+}-treated groups, the number of follicular cells gradually decreased with increasing Cd^{2+} concentrations (Figures 2B, C, E, G) and ovarian cells had a loose and more irregular arrangement (yellow arrows in Figures 2B, C, E, G) compared with the control group. Cadmium treatment caused the loss of gonadal tissue structure (rectangles in Figures 2B, C, E, G), with some ovarian cells being deformed in the group treated with 12 mg L^{-1} Cd^{2+} (Figures 2G–I). In addition, chromatin condensation, a typical apoptotic feature, was observed in the nucleus of ovarian cells of the higher Cd^{2+} treated groups (Figures 2D, F, H, I, red arrows). The size of the nucleus in the ovarian cells of the group treated with 12 mg L^{-1} Cd^{2+} was clearly smaller compared with the ovarian cells of 3 and 6 mg L^{-1} Cd^{2+}-treated groups (Figures 2D, F, H, I).

3.4 Detection of apoptosis

3.4.1 AO/EB staining

After AO/EB staining, four types of fluorescence cells were detected by fluorescence microscopy: green (normal live cells), yellow (early-stage apoptotic cells), orange (late-stage apoptotic cells), and red (dead cells) fluorescence cells (Figures 3A–E). The cells in the control group were normal live cells (Figure 3A), indicating no obvious apoptotic ovarian cells. As for the Cd^{2+}-treated groups, the number of early-stage and late-stage apoptotic cells increased significantly with increasing concentrations of Cd^{2+}, with the highest Cd^{2+} concentration resulting in the greatest number of orange-red fluorescence cells, indicating they were most severely damaged (Figures 3B–E).

The apoptotic rate of the ovarian cells was calculated according to the following formula: apoptosis rate = [(early-stage apoptotic cells + late-stage apoptotic cells)/total cells]×100%. The apoptotic rate for the control group was just 3.5%, while the apoptotic rate for the Cd^{2+}-treated groups increased significantly with increases in Cd^{2+} concentration, reaching 75.2% for the group treated with 12 mg·L^{-1} Cd^{2+} (Figure 3F). These results indicated that the rate of ovarian cell apoptosis was positively correlated with the Cd^{2+} concentration that the clams were exposed to.

3.4.2 Flow cytometry detection

The ovarian cells of *M. meretrix* were detected by flow cytometry after Annexin V-FITC/PI staining. The cells were distributed in four regions: Q1 (mechanically damaged cells), Q2 (late-stage apoptotic cells), Q3 (early-stage apoptotic cells), Q4 (normal cells) (Figures 4A–E). Compared with the control group, the number of normal cells in the Cd^{2+}-treated groups decreased significantly, while the number of late-stage apoptotic cells and early-stage apoptotic cells gradually increased with

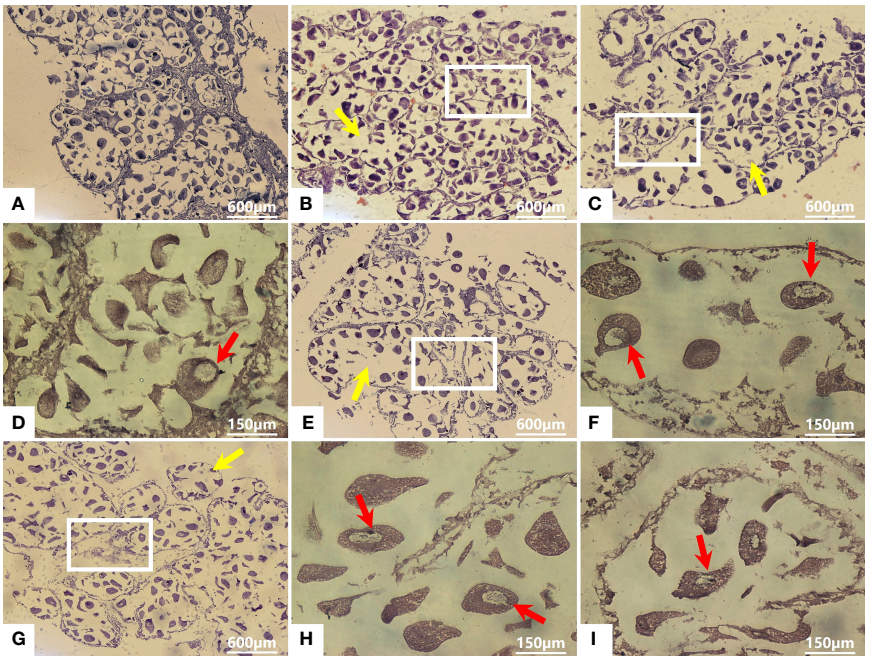

FIGURE 2
Histological sections of the ovary from *M. meretrix* that were subjected to Cd^{2+} and no Cd^{2+} treatments. Control group **(A)**; Groups treated with 1.5 mg L^{-1} Cd^{2+} **(B)**, 3 mg L^{-1} Cd^{2+} **(C, D)**, 6.0 mg L^{-1} Cd^{2+} **(E, F)**, and 12 mg L^{-1} Cd^{2+} **(G–I)**. Yellow arrows indicate the irregularly distributed ovarian cells. Red arrows indicate nuclear chromatin condensation. Rectangles indicate the loss of gonadal tissue structure.

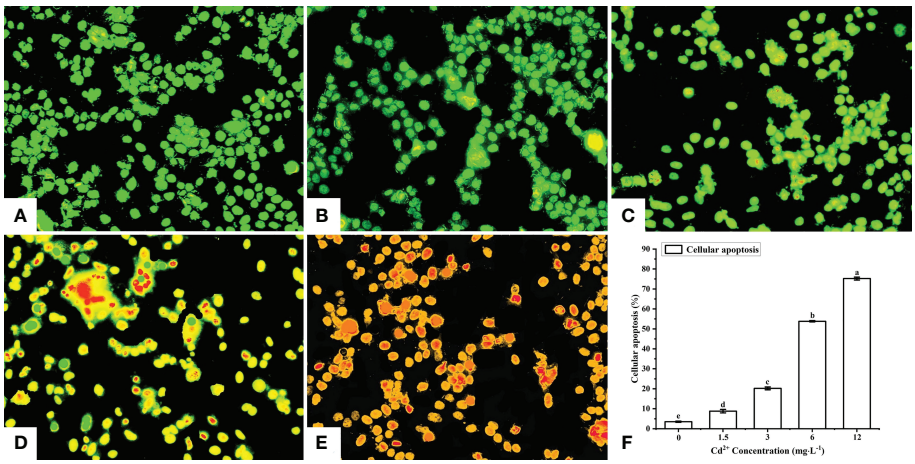

FIGURE 3
Detection of apoptotic *M. meretrix* ovarian cells by fluorescence microscopy following exposure to Cd^{2+}. **(A)** control group; **(B)** 1.5 mg L^{-1}; **(C)** 3 mg L^{-1}; **(D)** 6.0 mg L^{-1}; **(E)** 12 mg L^{-1} Cd^{2+} concentration. **(F)** The plot shows the rate of apoptosis in *M. meretrix* ovarian cells as determined from the microscopy data. Significant ($P < 0.05$) differences among groups are indicated by different letters above the bars in the plot.

increasing Cd^{2+} concentrations. This suggested that the apoptotic rate increased gradually with increases in Cd^{2+} concentration. The apoptotic rate of the ovarian cells for each group was calculated according to the data in the corresponding flow cytometry chart. A comparison of the apoptotic rates among the different groups revealed a significant increase for each Cd^{2+}-treated group relative to the control group (Figure 4F).

3.4.3 Effects of Cd on caspase-3, -8, -9 activities

Caspase-3, -8, -9 activity levels in the ovary of *M. meretrix* treated with Cd^{2+} increased gradually with increasing Cd^{2+} concentrations (Figures 5A–C). For caspase-3, there was no significant difference in activity between the control group and the groups treated with 1.5 mg L^{-1} and 3 mg L^{-1} Cd^{2+}, but the group treated with 6 mg L^{-1} and 12 mg L^{-1} Cd^{2+} exhibited a significantly ($P < 0.05$) higher activity than the control group (Figure 5A). For caspase-8, all Cd^{2+}-treated groups exhibited a significantly higher activity compared with the control group, but no significant difference was observed among the different Cd^{2+}-treated groups (Figure 5B). As for caspase-9, there was a significant ($P < 0.05$) difference in the activity between the control group and each Cd^{2+}-treated group (Figure 5C). Taken together, the data suggested that Cd^{2+} could enhance caspase activity, with different types of caspases having different cadmium sensitivities.

3.5 Effect of Cd on the mRNA expression levels of p53, MT, Bax, Bcl-2 and Caspase-3

The clams treated with Cd^{2+} showed a significantly higher level of *MT* mRNA than the control clams, but the initial increase was followed by a substantial decrease at the highest Cd^{2+} concentration (Figure 6A, white bars). The maximum level was found in the group treated with 3 mg L^{-1} Cd^{2+}, and it was significantly ($P < 0.05$) different from the control group and the groups treated with 1.5 and 12 mg L^{-1} Cd^{2+}. The level of *p53* mRNA increased with increasing Cd^{2+} concentrations (Figure 6A, black bars), but a significant increase over the control group was only detected for the groups treated with Cd^{2+} higher than 1.5 mg L^{-1}. Cadmium, therefore, appeared to induce the expression of p53 and MT in the ovary of *M. meretrix*, with a more obvious concentration effect seen in the case of p53 expression.

The level of *Bax* mRNA increased in a concentration-dependent manner after Cd^{2+} treatment (Figure 6B white bars), with the groups treated with 3, 6 and 12 mg L^{-1} Cd^{2+} all exhibited significantly ($P < 0.05$) higher levels than the control group, while there was no significant ($P > 0.05$) difference between the control group and the group treated with the lowest Cd^{2+} concentration. As for the level of *Bcl-2* mRNA, it increased for the group treated with 1.5 mg L^{-1} Cd^{2+} but then

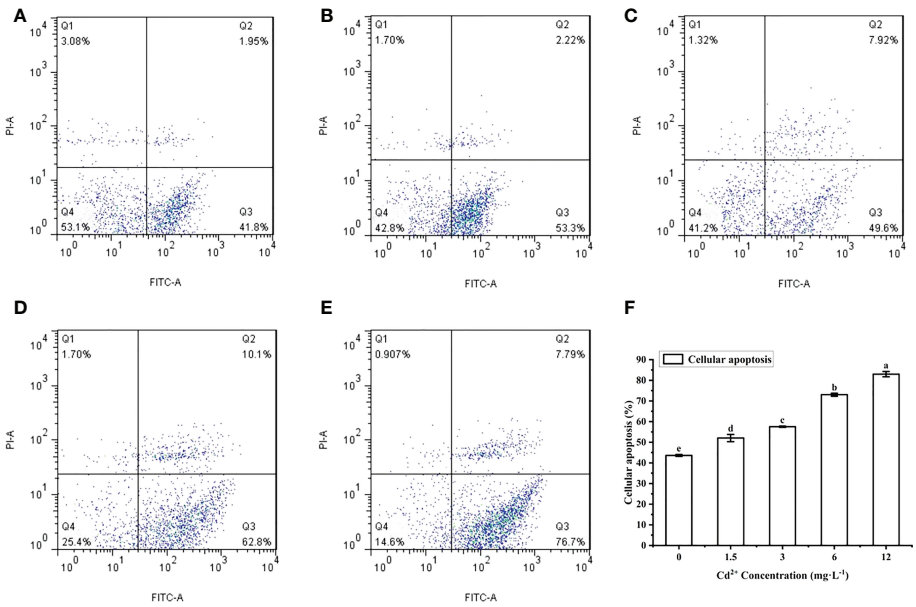

FIGURE 4
Detection of apoptosis in *M. meretrix* ovarian cells by flow cytometry. **(A)** control group; **(B)** 1.5 mg L^{-1}; **(C)** 3 mg L^{-1}; **(D)** 6.0 mg L^{-1}; and **(E)** 12 mg L^{-1} Cd^{2+} concentration. **(F)** The plot shows the rate of apoptosis in *M. meretrix* ovarian cells as determined from the flow cytometry data. Significant ($P < 0.05$) differences among groups are indicated by different letters above the bars in the plot.

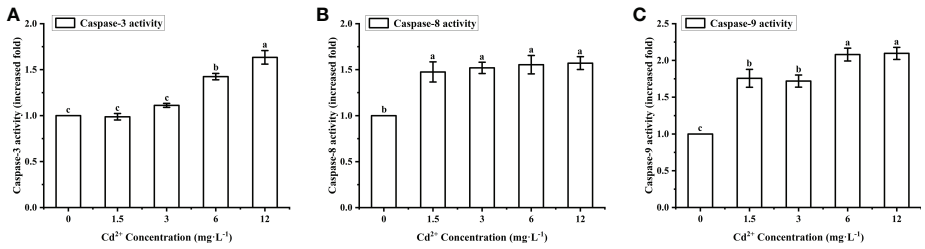

FIGURE 5
Effects of Cd on the activities of caspase-3, caspase-8 and caspase-9 in *M. meretrix* ovary. **(A)** Caspase-3; **(B)** caspase-8; **(C)** caspase-9. Different letters indicate significant ($P < 0.05$) differences among groups as revealed by Tukey's post-hoc multiple comparison tests; Data are expressed as means ± SE (n = 6).

decreased with increasing Cd^{2+} concentrations relative to the control group (Figure 6B black bars), and the difference in *Bcl-2* mRNA level between the control and each of the Cd^{2+}-treated group was significant ($P<0.05$). The level of *Caspase-3* mRNA increased with increasing Cd^{2+} concentrations and all Cd^{2+}-treated groups exhibited significantly ($P < 0.05$) higher levels than the control group (Figure 6C). This indicated an obvious degree of apoptosis in ovarian cells linked to the concentration effect of Cd^{2+}. Overall, the results did suggest that Cd^{2+} could activate the p53-mediated apoptosis pathway in ovarian cells, although the changes in these apoptosis-associated markers did not seem to have a consistent response to Cd^{2+} concentration.

3.6 Correlation analysis of *p53* mRNA with oxidative damage indexes and apoptosis-related factors

The *p53* mRNA level of the ovary was positively correlated with ROS, MDA, PCO, DPC and *MT, Bax* mRNA levels and negatively correlated with T-AOC and *Bcl-2* mRNA levels (Figure 7). This indicated that oxidative damage and p53 apoptosis pathway were mutually stimulating in the ovarian cells of Cd^{2+} treated *M. meretrix*, such that when the p53 apoptosis pathway was activated, the function of the intracellular antioxidant system may be inhibited.

4 Discussion

4.1 Toxic effects of cadmium on ovary

Aquatic environment is the final acceptor of various cadmium pollutions and cadmium can remain and become enriched in aquatic organisms in tissues such as the gonads, gills, foot and visceral mass for a long time through the food chain (Revathi et al., 2011; Nunez-Nogueira et al., 2012; Chen et al., 2020). If cadmium is accumulated in the gonads, it can result in serious reproductive toxicity (Fleege et al., 2003). Long-term exposure to cadmium can inhibit ovulation and affect the development of the embryo and larva of fish (Szczerbik et al., 2006; Wu et al., 2012). Therefore, it is of great significance to study the effect of cadmium on the ovary to better understand the relationship between aquatic ecological pollution and aquatic organisms. In this study, Cd^{2+} was found to accumulate in *M. meretrix* ovary in a concentration-dependent manner. This

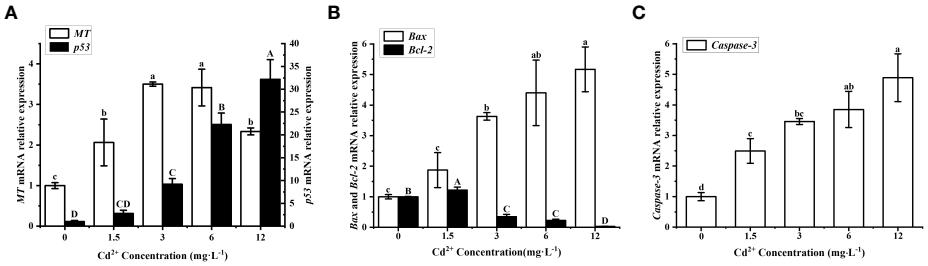

FIGURE 6
Effects of Cd on apoptotic markers in *M. meretrix* ovary. **(A)** *p53* (white bars) and *MT* mRNA (black bars); **(B)** *Bax* (white bars) and *Bcl-2* mRNA (black bars); **(C)** *Caspase-3* mRNA. Different letters indicate significant ($P < 0.05$) differences among groups as revealed by Tukey's post-hoc multiple comparison tests; Data are expressed as means ± SE (n = 6).

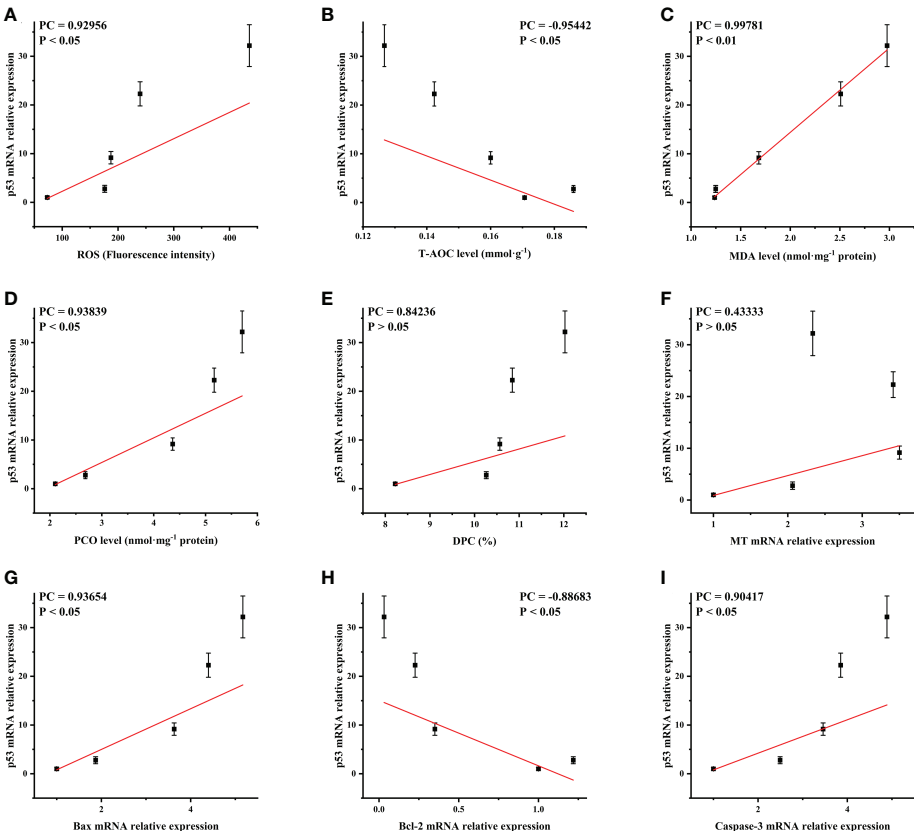

FIGURE 7
Correlation analysis of *p53* mRNA expression with the oxidative damage-related and apoptosis-related markers. Oxidative damaged-related markers: **(A)** ROS; **(B)** T-AOC; **(C)** MDA; **(D)** PCO; **(E)** DPC; **(F)** MT. Apoptosis-related factors: **(G)** Bax; **(H)** Bcl-2; **(I)** Caspase-3. PC, Pearson correlation coefficient.

finding is consistent with that of Chen et al. (2019) who found that exposure to Cd^{2+} led to a significant accumulation of Cd^{2+} in the ovary of *E. sinensis* in a concentration-dependent manner. Xu et al. (2016) also found the accumulation of cadmium in the ovary of the crab *Sinopotamon henanense* is time-dependent. Cd^{2+} toxicity has been comprehensively explored in many *in vitro* and *in vivo* studies, and various molecular and cellular mechanisms have been proposed to explain the toxicity of this metal. Among these mechanisms, oxidative stress is considered to play an important role (Matovic et al., 2015; Ren et al., 2019; Chen et al., 2020). The enrichment of cadmium to a certain level within an aquatic animal will lead to the production of a large amount of ROS (Gao et al., 2021; Wang et al., 2021). The increased extent of lipid peroxidation we observed in *M. meretrix* ovary manifested itself as increased ROS, MDA, DPC and PCO levels and decreased T-AOC and *MT* mRNA levels (Figure 1 & Figure 6A). Exposure to cadmium, therefore, led to the production of an excessive amount of ROS which subsequently induced lipid peroxidation in the ovary. The excess ROS can also cause the cross-linking of proteins, nucleic acids and other macromolecules, making them unable to carry out their normal functions in the ovarian cells, thereby adding further stress to the survival of the ovarian cells. The appearance of MDA, the final product of lipid peroxidation, could lead to the denaturation of the cell membrane (Gao et al., 2021). PCO is an irreversible protein modification that occurs under the action of oxidation, and such change in protein structure will result in the loss of the protein function (Fedorova et al., 2014). Other well-known forms of cellular damage induced by toxic agents are protein crosslinking and DNA fragmentation, commonly measured by the DPC assay (Jena, 2012; Cheng et al., 2021). In the case of *M. meretrix* ovary, DPC level was found to increase significantly in the group exposed to the lowest Cd^{2+} concentration (1.5 mg L^{-1}), however, the levels of MDA and PCO in this group were not significantly different from those of the control group (Figures 1A–C). This suggested that within the *M. meretrix* ovarian cells, DNA might be more sensitive to cadmium compared with lipids and proteins.

Excessive production of ROS can likely trigger an antioxidant defense response, which can subsequently work to purge the

system of these free radicals. Experimentally, the purging of free radicals is measured in terms of T-AOC. The rising level of T-AOC in *M. meretrix* ovary following Cd^{2+} exposure further demonstrated the ability of Cd^{2+} to promote the production of ROS in the cells. The rise in T-AOC was accompanied by a rising level of *MT* mRNA. Both T-AOC level and MT expression were stimulated by Cd^{2+}, but their increases appeared to drop at the higher ends of Cd^{2+} concentration (Figures 1D, 6A), suggesting that the antioxidant capacity of the ovary might have been overwhelmed or might have reached a maximum level. Similar findings have been reported for *E. sinensis* following exposure to Cd^{2+}, where the activities of antioxidant enzymes such as SOD, CAT and GPx were found to increase at lower Cd^{2+} concentrations but decreased at higher Cd^{2+} concentrations (Chen et al., 2019). This suggested that there could be a threshold to which the antioxidant capacity of the cells can deal with the rise in oxidative stress induced by an external agent, and the likelihood of the cells surviving the onslaught of oxidative stress is pretty much dependent on the upper threshold of the anti-oxidative response intrinsic to that organism.

The accumulation of free radicals caused by cadmium can inhibit the development of the ovary through affecting the normal morphology of the membrane system and cells (Xu et al., 2016). The accumulation of Cd^{2+} in *M. meretrix* ovary was also manifested as a severely damaged cellular structure revealed by microscopic examination (Figure 2). The normal survival of ovarian cells depends on the transport of substances from other tissues to these cells. Cadmium may enter the ovarian cells through the routes of material transport and accumulate in the cells, gradually increasing the survival pressure for the ovarian cells. Some ovarian cells were able to withstand the oxidative damage caused by cadmium and became deformed, and the distance between different ovarian cells became larger (Figure 2). Revathi et al. (2011) found that in cadmium-treated *Macrobrachium rosenbergii*, the ovary has both immature oocytes and hypertrophied primary oocytes with more vacuoles. When the fish *Oreochromis niloticus* was exposed to Cd^{2+} for 30 days, a seemingly increase in the number of primary follicles and secondary follicles was noticed in all Cd^{2+}-exposed female fish relative to the control, and after Cd^{2+} exposure for 60 days, deformed follicles were observed in the ovaries (Luo et al., 2015). Cadmium-treated rats have been shown to exhibit irregular morphology, vacuolated primary follicles and reduced luteal volume (da Costa et al., 2021). The number of primordial follicles and primary follicles in these rats was significantly lower than that in the control rats. Cadmium-induced destruction of ovarian tissue appears to be definite, universal and irreversible.

Patel et al. (2021) found that cadmium has a great toxic effect on the reproductive system, and this may consequently have a negative impact on the fertilization process, embryonic development and embryo survival rate. Cadmium can cause thinning of the ovarian cortical area, damage or loss of oocytes as well as reducing the growth and maturation of the follicles or turning them into vacuoles, thereby reducing the ovulation and fertilization ability in mammals (Thompson & Bannigan, 2008; Ikeh-Tawari et al., 2013). Wu et al. (2013) observed a 60% decrease in the mating rate for female zebrafish after exposure to 8.9–35.6 μM Cd^{2+} for 72 h. Likewise, cadmium exposure was found to result in a lower number of normal ovarian cells (Figures 2D–I), suggesting that cadmium may reduce ovulation in *M. meretrix*. The quality of the ovarian cells determines the success rate of fertilization and the normal development of the embryo. In addition, cadmium-induced DNA damage may affect the integrity of the genetic material carried by the ovarian cells, leaving a potential threat to embryonic development. Our previous study has found that cadmium exposure can disrupt the membranous structure of *M. meretrix* testis and significantly reduce sperm survival (Gao et al., 2021). In addition, the levels of Cd enrichment, ROS, MDA, DPC and PCO in the testis are also lower than those found in the ovary, although the number of normal sperm is significantly reduced in *M. meretrix* individuals exposed to increasing Cd^{2+} concentrations as in the case of the ovary observed in this study (Figures 1–4). This indicated that the ovary might have suffered a more serious degree of oxidative damage than the testis, consistent with Luo et al. (2015) who found that female tilapia is more sensitive to Cd than male tilapia. However, the number of ovarian cells in *M. meretrix* was much lower than that of sperm, and since the nutrients needed for embryonic development are mainly stored in the ovary, this could mean that the detrimental effects of reduced ovarian cell count and structural damage on *M. meretrix* reproduction may be greater than the adverse effects of reduced sperm count. In *M. meretrix*, fertilization of the ova takes place outside the body. This means that cadmium not only can affect the formation and survival of the sperms and eggs by entering the body tissues of *M. meretrix*, but it can also interfere with the fertilization process by directly affecting the sperms and eggs that were successfully released into seawater. Therefore, the damage to ovarian cells caused by cadmium could directly affect the fecundity and seedling rate of *M. meretrix*. Our result provided support for the notion that Cd might pose a significant threat to the reproduction of clams through its damaging impact on ovarian cells. Apart from the biological impact that cadmium can inflict on aquatic animals, cadmium exposure can also adversely affect the economics of shellfish aquaculture (Chen et al., 2020) by decreasing the reproductive potential of the animals, and hence their production output. However, further research is required to examine the effect of Cd on the reproduction potential of *M. meretrix* cultured in cadmium-polluted water.

4.2 Responses of the apoptosis pathway after Cd exposure

Apoptosis, a genetically controlled self-destructive process under stress, plays a crucial role in maintaining tissue

homeostasis by ridding the system of abnormal or damaging cells (Elmore, 2007; Xu and Yang, 2018). A large number of studies in recent years have shown that cadmium can induce apoptosis in many tissues and cells, which include rat osteoblasts (Zheng et al., 2020), duck ovaries (Cao et al., 2016), carp neutrophils (Sun et al., 2020), crab hepatopancreas (Cheng et al., 2021) and ovary (Chen et al., 2019), clam gill (Wang et al., 2021) and hepatopancreas (Xia et al., 2016), demonstrating that apoptosis is one of the important consequences of cadmium toxicity. The study of cadmium-induced apoptosis has, therefore, become a hot topic to unravel the toxicity of cadmium at the molecular level. According to the AO/EB and flow cytometry data, the number of apoptotic *M. meretrix* ovarian cells increased with an increase in Cd^{2+} exposure concentration, with the number of apoptotic cells accounting for more than half of the total cells number at the highest Cd^{2+} concentration used (Figures 3 & 4). This suggested the existence of a concentration-dependent relationship between the extent of apoptosis and the accumulation of cadmium, consistent with our previous study (Gao et al., 2021), where we showed that increasing the Cd^{2+} concentration to which *M. meretrix* is exposed can lead to a significant increase in the number of apoptotic sperm cells. Apoptosis induced by heavy metals is a very complex process, involving a series of pro-apoptotic genes and proteins, including the Src-family tyrosinase kinase, Bax, Fas and p53, and anti-apoptotic genes and related proteins such as Bcl-2 and Myc (Kurochkin et al., 2011; Jena, 2012). We have previously shown that in *M. meretrix* testis, Cd^{2+}-induced apoptosis can up-regulate the levels of ROS and caspase-3, -9 activities, while decreasing the levels of $\Delta\psi m$ and CCO activity, activating caspase signaling and triggering apoptosis, with p53 playing a vital role in the Cd^{2+}-induced apoptosis (Gao et al., 2021). Furthermore, Cd^{2+} was also found to induce apoptosis in clam gill *via* the mitochondrial caspase-dependent pathway (Wang et al., 2021). In vertebrates, many genes or proteins, such as the caspase family, p53, Bax and Bcl-2, are considered to be key factors in both pathways (Huang et al., 2017; Sun et al., 2020). Caspase activation plays a central role in the execution of apoptosis. Caspase-8 and Caspase-9 are key proteins of the extrinsic (Huang et al., 2017; Sun et al., 2020) and intrinsic (Ren et al., 2019; Cheng et al., 2021) pathways of apoptosis, respectively. However, apoptosis ultimately relies on caspase-3 to regulate endonucleases to promote DNA cleavage (Kumar, 2007). The activation of caspase-3, -8 and -9 in *M. meretrix* ovary demonstrated that both the intrinsic and extrinsic pathways were involved in the apoptosis (Figure 5). However, caspase-8 activity in the ovary appeared to be insensitive to Cd^{2+} concentration (Figure 5B). This suggested that the extrinsic pathway of apoptosis in the ovarian cells may have reached saturation. Instead, caspase-9 activity appeared to correlate with Cd^{2+} concentration (Figure 5C). It could also suggest that within a certain Cd^{2+} concentration range (1.5–12 mg L^{-1}), the extrinsic pathway of apoptosis was not significantly correlated with Cd^{2+} concentration, while the intrinsic pathway of apoptosis was positively correlated with Cd^{2+} concentration. Thus, under the Cd^{2+} concentrations used in this study, the intrinsic apoptotic pathway seemed to be the main route by which *M. meretrix* ovarian cells would undergo apoptosis.

Among the intrinsic apoptosis pathways, the mitochondrial pathway is the most classic apoptosis pathway. The Bcl-2 family controls the permeability of the mitochondrial membrane and is the main regulator of the mitochondrial apoptosis pathway, while p53 plays a key role in the regulation of the Bcl-2 family of proteins (Ostrakhovitch et al., 2016; Yamada and Yoshida, 2019). The expression of these apoptosis-related genes (*caspase-3, p53, Bcl-2* and *Bax*) was found to be regulated by Cd^{2+} (Figure 6). For example, after Cd^{2+} treatment, the level of Bcl-2 expression was decreased under higher Cd^{2+} concentrations (3-12 mg L^{-1}) while the levels of caspase-3, Bax and p53 expressions increased in a concentration-dependent manner. These results implied that elevation of ROS level could directly lead to DNA damage, and at the same time, it may also activate the mitochondrial-related apoptosis signaling pathway, such as by activating the expression of p53, triggering the expression of Bax. The activation of caspase-3 may be due to the direct effect of Cd^{2+} on Bax protein, which can subsequently induce mitochondrial membrane permeability with the consequent release of cytochrome c into the cytoplasm. Furthermore, the data also implied that Cd may deplete the level of mitochondrial Bcl-2 protein, and increase both the levels of caspase-3 activity and mRNA in *M. meretrix* ovary, probably partly because of an increase in the amount of ROS. The positive correlations observed between p53 and each of the oxidative damage indexes and apoptosis-related factors (Figure 7) indicated the important role of p53 in mediating Cd^{2+}-induced apoptosis in *M. meretrix* ovarian cells.

5 Conclusion

In summary, this study demonstrated that cadmium exposure could lead to Cd^{2+} accumulation in *M. meretrix* ovary, which ultimately translated into increased oxidative damage as evidenced by the elevated MDA, DPC and PCO levels and the reduced T-AOC level. At higher Cd^{2+} concentrations, the capacities of MT and T-AOC were unable to deal with the rising level of ROS to neutralize the Cd^{2+} toxicity. In addition to the mounting level of oxidative stress, Cd^{2+} also induced apoptosis in *M. meretrix* ovarian cells through both the intrinsic and extrinsic pathways, which involved the induction of *p53* and other apoptosis-related genes. The toxicity sustained by *M. meretrix* ovarian cells implied that clams raised in water polluted by Cd^{2+} might lead to a loss of fecundity, adversely affecting fertilization and embryo development, which could eventually translate into an economic loss.

Data availability statement

The original contributions presented in the study are included in the article/supplementary material. Further inquiries can be directed to the corresponding authors.

Ethics statement

The research article ensures objectivity and transparency in research and secures that accepted principles of ethical and professional conduct have been followed. This original research article does not contain any studies with human participants performed by any of the authors.

Author contributions

BB and YY were responsible for the experimental design, carrying out the experiments, data processing, and article writing. JW, QZ and MW performed the sample collection, sample processing and extraction. AC and XY provided experimental guidance and supervision. All authors contributed to the article and approved the submitted version.

Funding

This study was supported by the National Natural Science Foundation of China under Grant number 32071514 (to XY), the Nature Science Foundation of Zhejiang Province (CN) under Grant number LY18C030005 (to XY), the Innovation Program of Wenzhou University under Grant number JWXC2021104 (to YY) and the Student Innovation Training Project of Zhejiang province under Grant number 2021R (to JW).

Conflict of interest

The authors declare that the research was conducted in the absence of any commercial or financial relationships that could be construed as a potential conflict of interest.

Publisher's note

All claims expressed in this article are solely those of the authors and do not necessarily represent those of their affiliated organizations, or those of the publisher, the editors and the reviewers. Any product that may be evaluated in this article, or claim that may be made by its manufacturer, is not guaranteed or endorsed by the publisher.

References

Alyahya, H., Elgendy, A. H., Farraj, S. A., and Elhedeny, M. (2011). Evaluation of heavy metal pollution in the arabian gulf using the clam meretrix meretrix linnaeus 1758. *Water Air Soil Pollut.* 214, 499–507. doi: 10.1007/s11270-010-0441-x

Amiard, J. C., Amiard-Triquet, C., Barka, S., Pellerin, J., and Rainbow, P. S. (2006). Metallothioneins in aquatic invertebrates: Their role in metal detoxification and their use as biomarkers. *Aquat. Toxicol.* 76, 160–202. doi: 10.1016/j.aquatox.2005.08.015

Boudet, L. N. C., Polizzi, P., Romero, M. S., Robles, A., Marcovecchio, J. E., and Gerpe, M. S. (2015). Histopathological and biochemical evidence of hepatopancreatic toxicity caused by cadmium in white shrimp, *Palaemonetes argentinus*. ecotoxicol. *Environ. Saf.* 113, 231–240. doi: 10.1016/j.ecoenv.2014.11.019

Brady, C. A., and Attardi, L. D. (2010). p53 at a glance. *J. Cell Sci.* 123, 2527–2532. doi: 10.1242/jcs.064501

Cao, R. W., Liu, Y. L., Wang, Q., Zhang, Q. Q., Yang, D. L., Liu, H., et al. (2018). The impact of ocean acidification and cadmium on the immune responses of pacific oyster, *Crassostrea gigas*. *Fish Shellfish Immunol.* 81, 456–462. doi: 10.1016/j.fsi.2018.07.055

Cao, H. B., Xia, B., Zhang, M. M., Liao, Y. L., Yang, Z., Hu, G. L., et al. (2016). Changes of antioxidant function and the mRNA expression levels of apoptosis genes in duck ovaries caused by molybdenum or/and cadmium. *Biol. Trace Elem. Res.* 171, 410–418. doi: 10.1007/s12011-015-0514-1

Cekic, S. D., Cetinkaya, A., Avan, A. N., and Apak, R. (2013). Correlation of total antioxidant capacity with reactive oxygen species (ROS) consumption measured by oxidative conversion. *J. Agric. Food Chem.* 61, 5260–5270. doi: 10.1021/jf3051297

Cheng, C. H., Ma, H. L., Deng, Y. Q., Feng, J., Jie, Y. K., and Guo, Z. X. (2021). Oxidative stress, cell cycle arrest, DNA damage and apoptosis in the mud crab (*Scylla paramamosain*) induced by cadmium exposure. *Chemosphere* 263. doi: 10.1016/j.chemosphere.2020.128277

Chen, R. Q., Ye, F. Y., Lin, J. H., Zhou, J. Y., Cai, J. J., and Ying, X. P. (2019). Effects of cadmium and mercury on oxidative stress indexes in the ovary of *Eriocheir sinensis*. *Acta Hydrobiologica Sin.* 43, 554–562. doi: 10.7541/2019.067

Chen, M. X., Zhou, J. Y., Lin, J. H., Tang, H. C., Shan, Y. F., Chang, A. K., et al. (2020). Changes in oxidative stress biomarkers in *Sinonovacula constricta* in response to toxic metal accumulation during growth in an aquaculture farm. *Chemosphere* 248. doi: 10.1016/j.chemosphere.2020.125974

da Costa, C. S., Oliveira, T. F., Freitas-Lima, L. C., Padilha, A. S., Krause, M., Carneiro, M., et al. (2021). Subacute cadmium exposure disrupts the hypothalamic-pituitary-gonadal axis, leading to polycystic ovarian syndrome and premature ovarian failure features in female rats. *Environ. Pollut.* 269. doi: 10.1016/j.envpol.2020.116154

Das, S., and Mukherjee, D.. (2013). Effect of cadmium chloride on secretion of 17 beta-estradiol by the ovarian follicles of common carp, Cyprinus carpio. *Gen. Comp. Endocr.* 181, 107–114. doi: 10.1016/j.ygcen.2012.10.010

Elmore, S. (2007). Apoptosis: A review of programmed cell death. *Toxicol. Pathol.* 35, 495–516. doi: 10.1080/01926230701320337

Fedorova, M., Bollineni, R. C., and Hoffmann, R. (2014). Protein carbonylation as a major hallmark of oxidative damage: update of analytical strategies. *Mass Spectrom. Rev.* 33, 79–97. doi: 10.1002/mas.21381

Fleeger, J. W., Carman, K. R., and Nisbet, R. M. (2003). Indirect effects of contaminants in aquatic ecosystems. *Sci. Total Environ.* 317, 207–233. doi: 10.1016/s0048-9697(03)00141-4

Gao, Y. L., Hong, J. M., Guo, Y. K., Chen, M. X., Chang, A. K., Xie, L., et al. (2021). Assessment spermatogenic cell apoptosis and the transcript levels of metallothionein and p53 in *Meretrix meretrix* induced by cadmium. ecotoxicol. *Environ. Saf.* 217. doi: 10.1016/j.ecoenv.2021.112230

Garriz, A., del Fresno, P. S., Carriquiriborde, P., and Miranda, L. A. (2019). Effects of heavy metals identified in chascomus shallow lake on the endocrine-reproductive axis of pejerrey fish (*Odontesthes bonariensis*). *Gen. Comp. Endocr.* 273, 152–162. doi: 10.1016/j.ygcen.2018.06.013

Gu, B. N., Liang, W., Yang, T. Z., Hu, Z. J., and Shen, H. D. (2019). Metallothionein, hemocyte status and superoxide dismutase/aspartate aminotransferase activity are sensitive biomarkers of cadmium stress in *Onchidium reevesii*. aquat. *Toxicol* 215. doi: 10.1016/j.aquatox.2019.105284

Huang, M. Y., Su, L., Yang, L. M., Zhu, L. L., Liu, Z. W., and Duan, R. Y. (2017). Effect of exogenous TGF-beta 1 on the cadmium-induced nephrotoxicity by inhibiting apoptosis of proximal tubular cells through PI3K-AKT-mTOR signaling pathway. *Chem. Biol. Interact.* 269, 25–32. doi: 10.1016/j.cbi.2017.03.010

Huang, Y., Tang, H. C., Jin, J. Y., Fan, M. B., Chang, A. K., and Ying, X. P. (2020). Effects of waterborne cadmium exposure on its internal distribution in *Meretrix meretrix* and detoxification by metallothionein and antioxidant enzymes. *Front. Mar. Sci.* 7. doi: 10.3389/fmars.2020.00502

Ikeh-Tawari, E. P., Anetor, J. I., and Charles-Davies, M. A. (2013). Cadmium level in pregnancy, influence on neonatal birth weight and possible amelioration by some essential trace elements. *Toxicol. Int.* 20, 108–112. doi: 10.4103/0971-6580.111558

Jena, N. R. (2012). DNA Damage by reactive species: Mechanisms, mutation and repair. *J. Biosci.* 37, 503–517. doi: 10.1007/s12038-012-9218-2

Kim, B., Srivastava, S. K., and Kim, S. H. (2015). Caspase-9 as a therapeutic target for treating cancer. *Expert Opin. Ther. Tar.* 19, 113–127. doi: 10.1517/14728222.2014.961425

Kumar, S. (2007). Caspase function in programmed cell death. *Cell Death Differ.* 14, 32–43. doi: 10.1038/sj.cdd.4402060

Kurochkin, I. O., Etzkorn, M., Buchwalter, D., Leamy, L., and Sokolova, I. M. (2011). Top-down control analysis of the cadmium effects on molluscan mitochondria and the mechanisms of cadmium-induced mitochondrial dysfunction. *Am. J. Physiol. Regul. Integr. Comp. Physiol.* 300, R21–R31. doi: 10.1152/ajpregu.00279.2010

Lin, Y., Huang, J. J., Dahms, H. U., Zhen, J. J., and Ying, X. P. (2017). Cell damage and apoptosis in the hepatopancreas of *Eriocheir sinensis* induced by cadmium. *Aquat. Toxicol.* 190, 190–198. doi: 10.1016/j.aquatox.2017.07.008

Livak, K. J., and Schmittgen, T. D. (2001). Analysis of relative gene expression data using real-time quantitative PCR and the 2(T)(-delta delta c) method. *Methods* 25, 402–408. doi: 10.1006/meth.2001.1262

Luo, Y. J., Shan, D., Zhong, H., Zhou, Y., Chen, W. Z., Cao, J. L., et al. (2015). Subchronic effects of cadmium on the gonads, expressions of steroid hormones and sex-related genes in tilapia *Oreochromis niloticus*. *Ecotoxicology* 24, 2213–2223. doi: 10.1007/s10646-015-1542-5

Matovic, V., Buha, A., Dukic-Cosic, D., and Bulat, Z. (2015). Insight into the oxidative stress induced by lead and/or cadmium in blood, liver and kidneys. *Food Chem. Toxicol.* 78, 130–140. doi: 10.1016/jict.2015.02.011

Nunez-Nogueira, G., Fernandez-Bringas, L., Ordiano-Flores, A., Gomez-Ponce, A., de Leon-Hill, C. P., and Gonzalez-Farias, F. (2012). Accumulation and regulation effects from the metal mixture of zn, Pb, and cd in the tropical shrimp *Penaeus vannamei*. biol. *Trace Elem. Res.* 150, 208–213. doi: 10.1007/s12011-012-9500-z

Ostrakhovitch, E. A., Song, Y. P., and Cherian, M. G. (2016). Basal and copper-induced expression of metallothionein isoform 1,2 and 3 genes in epithelial cancer cells: The role of tumor suppressor p53. *J. Trace Elem. Med. Biol.* 35, 18–29. doi: 10.1016/j.jtemb.2016.01.008

Patel, N., Chauhan, D., Shahane, S., Rai, D., Ali Khan, M. Z., Mishra, U., et al. (2021). "Contamination and health impact of heavy metals," in *Water pollution and remediation: Heavy metals*. Eds. Inamuddin,, M. I. Ahamed and E. Lichtfouse (Cham: Springer International Publishing), 259–280.

Ren, X. Y., Wang, X., Liu, P., and Li, J. (2019). Bioaccumulation and physiological responses in juvenile *Marsupenaeus japonicus* exposed to cadmium. *Aquat. Toxicol.* 214. doi: 10.1016/j.aquatox.2019.105255

Revathi, P., Vasanthi, L. A., and Munuswamy, N. (2011). Effect of cadmium on the ovarian development in the freshwater prawn *Macrobrachium rosenbergii* (De man). *Ecotoxicol. Environ. Saf.* 74, 623–629. doi: 10.1016/j.ecoenv.2010.08.027

Sarban, S., Kocyigit, A., Yazar, M., and Isikan, U. E. (2005). Plasma total antioxidant capacity, lipid peroxidation, and erythrocyte antioxidant enzyme activities in patients with rheumatoid arthritis and osteoarthritis. *Clin. Biochem.* 38, 981–986. doi: 10.1016/j.clinbiochem.2005.08.003

Sevcikova, M., Modra, H., Slaninova, A., and Svobodova, Z. (2011). Metals as a cause of oxidative stress in fish: A review. *Vet. Med-Czech* 56, 537–546. doi: 10.17221/4272-vetmed

Sun, J. X., Wang, S. C., Cao, Y. R., Wang, S. T., and Li, S. (2020). Cadmium exposure induces apoptosis, inflammation and immunosuppression through CYPs activation and antioxidant dysfunction in common carp neutrophils. *Fish Shellfish Immunol.* 99, 284–290. doi: 10.1016/j.fsi.2020.02.015

Szczerbik, P., Mikolajczyk, T., Sokolowska-Mikolajczyk, A., Socha, M., Chyb, J., and Epler, P. (2006). Influence of long-term exposure to dietary cadmium on growth, maturation and reproduction of goldfish (subspecies: Prussian carp *Carassius auratus gibelio* b.). *Aquat. Toxicol.* 77, 126–135. doi: 10.1016/j.aquatox.2005.11.005

Thompson, J., and Bannigan, J. (2008). Cadmium: Toxic effects on the reproductive system and the embryo. *Reprod. Toxicol.* 25, 304–315. doi: 10.1016/j.reprotox.2008.02.001

Tirani, M. M., and Haghjou, M. M. (2019). Reactive oxygen species (ROS), total antioxidant capacity (AOC) and malondialdehyde (MDA) make a triangle in evaluation of zinc stress extension. *J. Anim. Plant Sci-Pak.* 29, 1100–1111.

Tummers, B., and Green, D. R. (2017). Caspase-8: regulating life and death. *Immunol. Rev.* 277, 76–89. doi: 10.1111/imr.12541

Wang, J. H., Deng, W. F., Zou, T., Bai, B. B., Chang, A. K., and Ying, X. P. (2021). Cadmium-induced oxidative stress in *Meretrix meretrix* gills leads to mitochondria-mediated apoptosis. *Ecotoxicology* 30, 2011–2023. doi: 10.1007/s10646-021-02465-8

Wang, G. W., Klein, J. B., and Kang, Y. J. (2001). Metallothionein inhibits doxorubicin-induced mitochondrial cytochrome c release and caspase-3 activation in cardiomyocytes. *J. Pharmacol. Exp. Ther.* 298, 461–468.

Wang, L., Xu, T., Lei, W. W., Liu, D. M., Li, Y. J., Xuan, R. J., et al. (2011). Cadmium-induced oxidative stress and apoptotic changes in the testis of freshwater crab, *Sinopotamon henanense*. *PloS One* 6. doi: 10.1371/journal.pone.0027853

Wu, S. M., Jong, K. J., and Lee, Y. J. (2006). Relationships among metallothionein, cadmium accumulation, and cadmium tolerance in three species of fish. *Bull. Environ. Contam. Toxicol.* 76, 595–600. doi: 10.1007/s00128-006-0961-7

Wu, S. M., Tsai, P. J., Chou, M. Y., and Wang, W. D. (2013). Effects of maternal cadmium exposure on female reproductive functions, gamete quality, and offspring development in zebrafish (*Danio rerio*). *Arch. Environ. Contam. Toxicol.* 65, 521–536. doi: 10.1007/s00244-013-9909-1

Wu, S. M., Tsai, P. R., and Yan, C. J. (2012). Maternal cadmium exposure induces mt2 and smtB mRNA expression in zebrafish (*Danio rerio*) females and their offspring. *Comp. Biochem. Physiol. C Toxicol. Pharmacol.* 156, 1–6. doi: 10.1016/j.cbpc.2012.02.001

Xia, L. P., Chen, S. H., Dahms, H. U., Ying, X. P., and Peng, X. (2016). Cadmium induced oxidative damage and apoptosis in the hepatopancreas of *Meretrix meretrix*. *Ecotoxicology* 25, 959–969. doi: 10.1007/s10646-016-1653-7

Xie, J. F., Fan, R. J., and Meng, Z. Q. (2007). Protein oxidation and DNA-protein crosslink induced by sulfur dioxide in lungs, livers, and hearts from mice. *Inhal. Toxicol.* 19, 759–765. doi: 10.1080/08958370701399885

Xu, P., Chen, H., Xi, Y., Mao, X., and Wang, L. (2016). Oxidative stress induced by acute and sub-chronic cadmium exposure in the ovaries of the freshwater crab *Sinopotamon henanense* (DAI 1975). *Crustaceana* 89, 1041–1055. doi: 10.1163/15685403-00003573

Xu, Y. R., and Yang, W. X. (2018). Roles of three Es-caspases during spermatogenesis and cadmium-induced apoptosis in *Eriocheir sinensis*. *Aging-Us* 10, 1146–1165. doi: 10.18632/aging.101454

Yamada, K., and Yoshida, K. (2019). Mechanical insights into the regulation of programmed cell death by p53 *via* mitochondria. *Biochim. Biophys. Acta Mol. Cell Res.* 1866, 839–848. doi: 10.1016/j.bbamcr.2019.02.009

Zhang, Q. S., Zhang, M., Huang, X. J., Liu, X. J., and Li, W. P. (2016). Inhibition of cytoskeletal protein carbonylation may protect against oxidative damage in traumatic brain injury. *Exp. Ther. Med.* 12, 4107–4112. doi: 10.3892/etm.2016.3889

Zhan, J., Wang, S., Li, F., Ji, C., and Wu, H. (2021). Global characterization of dose-dependent effects of cadmium in clam *Ruditapes philippinarum*. *Environ. Pollut. (Barking Essex: 1987)* 273, 116443–116443. doi: 10.1016/j.envpol.2021.116443

Zheng, J. M., Zhuo, L. L., Ran, D., Ma, Y. G., Luo, T. W., Zhao, H. Y., et al. (2020). Cadmium induces apoptosis *via* generating reactive oxygen species to activate mitochondrial p53 pathway in primary rat osteoblasts. *Toxicology* 446. doi: 10.1016/j.tox.2020.152611